ANALYSIS OF STERIC PARTITION BEHAVIOR OF MOLECULES IN MEMBRANES USING STATISTICAL PHYSICS

Application to Gel Chromatography and Electrophoresis

JAN E. SCHNITZER
Department of Cell Biology, Yale University School of Medicine, New Haven, Connecticut 06510

ABSTRACT The principles of statistical physics are used to formulate general expressions for the steric partition behavior of molecules in both random and ordered membrane structures that may be applied to any shape of the solute and/or the volume-excluding element of the membrane. These expressions fully define partitioning in terms of the volume excluded to point molecules and to finite-sized molecules. The mean effective exclusion volume for a molecule is calculated as a function of a global interaction energy, which varies with position, conformation, and orientation of the molecule. It allows consideration of electrostatic and other nonsteric factors. To test the model, specific partition functions are derived for several simple geometries describing the membrane and solute. Frequently, the derived expressions agree with past analyses; however, a new expression describing partitioning within an random network of fibers is derived. It agrees with past results only in the limit of low exclusion volumes. With greater volume exclusions, past results greatly overestimate the partition function. It is applied to gel electrophoresis and chromatography and survives testing with available experimental data. Unlike past analyses, it predicts nonlinear Ferguson plots for agarose gel electrophoresis. In addition, an analytical expression predicting the minimum radius of a sphere excluded from a random fiber matrix is derived, tested, and found to agree with experimental data.

INTRODUCTION

The understanding of the physicochemical basis of the partitioning of molecules within membrane compartments containing volume-excluding elements is fundamental to many biophysical processes. Many biochemical fractionation techniques such as gel-exclusion chromatography, ultrafiltration, cell separation, and dialysis rely on the differential penetration of molecules or cells into porous volume-excluding membranes (1). The partition function is essential in interpreting elution volumes in size exclusion chromatography (2, 3), Ferguson plots in gel electrophoresis (3, 4), and molecular transport across filtration membranes and through solutions of macromolecules (5). In addition, partitioning of molecules within restrictive volumes strongly influences transmembrane transport through lipid membranes and ion channels (6–8), intracellular diffusion and convection through cytoplasm (9), intracellular compartmentalization of macromolecules (10), transcapillary exchange (11, 12), and receptor–ligand interactions at cell membrane surfaces (i.e., lipid polar region or the glycocalyx) (7, 12–14). The equilibrium distribution coefficient (partition function) of macromolecules between the bulk and membrane phase must be known in order to characterize these systems.

For many years the steric partition behavior of molecules in these types of restrictive environments has been predicted from the Ogston theory. Ogston derived an expression describing the distribution of spaces available to a spherical molecule in a random network of cylindrical fibers (15). Laurent and Killander (2) used Ogston's probability equation to determine the partition function of a sphere in random fiber matrix. Elegant work by Giddings et al. (16) confirmed the results of Ogston. They utilized statistical mechanics to derive more general solutions of the partition function for rigid macromolecules of various shapes by integrating the configurational probability function of these molecules over position and orientation space.

Extension of the theory based on the models of both Ogston (15) and Giddings et al. (16) (OG theory) has become the foundation for understanding the physical basis of size exclusion chromatography (2, 3) and gel electrophoresis (3, 4) These models are realistic in terms of known polymer structures such as agarose, cross-linked dextran, starch, hyaluronic acid, and polyacrylamide. Application to gel electrophoresis predicts constant retardation coefficients and linear Ferguson plot (log [mobility]) vs. gel concentration where mobility is defined as the migration rate per electric field strength) for all types of

molecules and gels (3). However, in contrast to this prediction, recent evidence indicates that Ferguson plots for various molecules and gels types are in fact nonlinear (17–21). Linearity within Ferguson plots may exist only within defined gel concentrations (17–19). Recently this nonlinear behavior has been explained empirically with adjustments of parameters contained within the Ogston theory (20, 21).

In this analysis, I will utilize statistical physics to describe the exclusion of molecules within porous membranes. Expressions for the partition behavior of molecules in both random and ordered membrane structures are derived rigorously. A general expression applicable to any geometry of both the permeating molecule and the volume-excluding element is derived and applied to give specific expressions for various simple geometries. These analytical expressions frequently agree with past analyses; however, important exceptions are found. For a membrane consisting of a random network of rodlike fibers, the analytical results approach the results of the OG theory and its extensions only in the limit of very low exclusion volumes. With higher exclusion volumes the OG theory greatly overestimates the partition function. This new model is applied to gel chromatography and electrophoresis. It is tested and shown to agree with available experimental data from both molecular mobility studies during gel electrophoresis and molecular partition behavior (i.e., elution volumes) during gel chromatography. Depending on the molecular dimensions of both the gel fiber and the permeant molecule, this analysis unlike the OG theory predicts nonlinear Ferguson plots with the retardation coefficient varying with gel concentration. In addition, an analytical expression predicting the maximum radius of a spherical particle entering a gel is derived, tested, and found to agree with available experiment results.

MATHEMATICAL ANALYSIS

The partition behavior of any molecule between two volumes in equilibrium is dependent on the change in free energy between the two phases. From a statistical standpoint, the ratio of the number of accessible states available to a molecule between two volumes in equilibrium equals the partition function ($\Phi = C_1/C_2$, where C is the concentration in volume 1 or 2). A state is accessible if the energy of that state is favorable relative to the thermal energy.

General Statistical Analysis of Accessible States

The mean number of accessible states (Ω_m^0) available to an imaginary point equivalent particle without charge of no size (radius, $r = 0$) within any volume is directly related to the total free volume (v_f^0, normalized as free volume per unit total volume) available to that molecule so that

$$\Omega_m^o = v_f^o \Omega_t^o, \tag{1}$$

where the superscript o denotes the zero molecular radius and the subscript t denotes the total possible number per volume in a given solution without significant exclusion.

Eq. 1 can be proved rigorously by considering a macroscopic system of solute particles dissolved in a solvent treated as a continuum. Dividing a unit volume into a large number of identical ensemble volumes, we can enumerate the likelihood that each ensemble can manifest its maximum number of accessible states. Within any ensemble volume the possible number of distinct accessible states for any molecule (Ω) is related to the ensemble number of molecules (n) and the number (N) of available positions for each molecule in the volume so that[1]

$$\Omega = \frac{N(N-1)(N-2)\ldots(N-n+1)}{n!} = \frac{N!}{n!(N-n)!} \rightarrow N, \quad \text{if } n = 1. \tag{2}$$

If the representative ensemble volume only contains 1 molecule ($n = 1$), Eq. 2 reduces to its simplest form. As the molecular concentration increases, the more precise factorial expression in Eq. 2 must be used.

In the membrane phase, N is calculated for a single conformation of the volume-excluding element in the ensemble volume. Within an ensemble volume the molecules potentially may be arranged and oriented (which constitutes a state) in a manner that either does or does not overlap with any exclusion element contained in the ensemble volume. The number of available positions (N) that do not overlap and the number of positions (N') that do potentially overlap equal the total number of possible positions (N_t, which as per Eq. 2 equals Ω_t) or $N + N' = N_t$. If this equation is divided by N_t, one gets the probability ($p = N/N_t$) that any single coordinate position within the ensemble volume is available for a point molecule (i.e., does not overlap with the volume-excluding element) and the probability ($q = N'/N_t$) that any one position is not accessible because of overlap with the volume-excluding element. Since each state is statistically independent, the probability ($P(N)$) that N of the N_t possible positions are accessible is dependent on p and q ($=1 - p$) in the form of a binomial distribution:

$$P(N) = \frac{N_t!}{N!(N_t - N)!} p^N (1-p)^{N_t - N}. \tag{3}$$

For a point molecule, N_t must be large so that the binomial distribution reduces to a gaussian distribution that allows

[1] (*a*) The n factorial in the denominator corrects for the fact that each particle is not distinct and is equivalent to the other; therefore, a switch of positions by two particles does not constitute a new accessible state. (*b*) In developing Eq. 2, the solvent is assumed to be a continuous medium and not particulate in nature. A more exact treatment in terms of solvent particles (in addition to the solute molecules which greatly increases both N and n) is possible, but the loss in simplicity and clarity would probably not be regained in predictive ability.

calculation of the mean value of N denoted by N_m as

$$N_m = \sum_{N=0}^{N_t} [P(N)N] = N_t P. \quad (4)$$

Analysis for a Point Molecule

For a single point molecule of infinitesimal size in a prescribed location within any volume the probability (p) that it is does not overlap with the volume-excluding element is just related to the available free volume (v_f^0) or the volume excluded (v_e^0) to that point molecule:

$$p = v_f^0 = 1 - v_e^0. \quad (5)$$

Eqs. 2, 4, and 5 give the mean number of accessible states (Ω_m^0) for point molecules as

$$\Omega_m^0 = \frac{(N_t^0 p)!}{n!(N_t^0 p - n)!} = N_t^0 p = \Omega_t^0 v_f^0, \quad (6)$$

which agrees with Eq. 1 and proves the intuitively obvious result that the number of accessible states for a point molecule in any volume is proportional to the free volume available.

From Eqs. 1 and 6 it is evident that for point molecules partitioning between two compartments the ratio of the number of accessible states within each volume is simply the change in free volume or exclusive volume from one volume to another. Therefore, the mean number of accessible states available to a point molecule within a membrane or gel (Ω_g^0) depends on the available free volume within the membrane or gel phase (g) relative to the volume available in the bulk solution (b) so that

$$\Omega_g^0/\Omega_b^0 = v_{fg}^0/v_{fb}^0 = 1 - \Delta v_f^0/v_{fb}^0 = 1 - \Delta v_e^0/v_{fb}^0, \quad (7)$$

where the change in free volume ($\Delta v_f^0 = v_{fb}^0 - v_{fg}^0$) or in exclusion volume ($\Delta v_e^0 = v_{eg}^0 - v_{eb}^0$) is relative to the free volume in the bulk solution. Eq. 7 defines the partition function for a point molecule (Φ^0) between two phases or compartments. When the reference compartment, in this case the bulk solution, is without significant volume exclusion or molecular self-exclusion from high solution concentrations, Eq. 7 yields

$$\Phi^0 = \Omega_g^0/\Omega_b^0 = 1 - v_{eg}^0, \quad (8)$$

which, if only steric interactions exist, may be interpreted as a loss in entropy relative to the bulk solution. As v_e^0 approaches 1, the accessible states ratio is zero and as v_e^0 approaches 0, the ratio becomes 1 with equal accessible states in both volumes.

Analysis of Molecules of Finite Size

The analysis is more complex for a molecule of finite size. Using the same general approach as above, the accessible states or availability of positions for point molecules and molecules of finite size can be compared. Any molecule of finite size can exist at any position available to a point molecule as given by Eq. 8 (for $r = 0$) unless it overlaps with the volume-excluding element. A particle of finite size has a maximum number of possible locations/accessible states (Ω_m^r) within a unit volume containing an exclusion element. If the volume exclusion element is structured in a fixed, regular order, a typical ensemble volume may be chosen. Let $\Gamma(w)$ be the probability that w positions or states (out of Ω_m states) are still accessible if a finite size molecule in any single conformation replaces the imaginary point molecule so that

$$\Gamma(w) = \frac{\Omega_m!}{w!\,(\Omega_m - w)!} p_r^w (1 - p_r)^{(\Omega_m - w)}, \quad (9)$$

where p_r is the probability that any single position available to a point molecule is also available to a finite size molecule since the exclusion volume element does not overlap with the volume of the molecule centered at this position. Obviously, the volume located near the surface of the volume excluding element is available to all point size molecules but is not available to finite size molecules because of steric exclusion from overlap. The ratio of the free volume available to the finite size molecule (v_f^r) relative to the point molecule is equal to p_r so that the single-state dependency equation is

$$p_r = v_f^r/v_f^0 = 1 - \Delta v_f^r/v_f^0 = 1 - \Delta v_e^r/v_f^0, \quad (10)$$

where $\Delta v_f^r = v_f^0 - v_f^r$ and $\Delta v_e^r = v_e^r - v_e^0$. For large values of Ω_m, the binomial distribution given by Eq. 9 reduces to a gaussian distribution so that

$$\Omega_m^r = \Omega_m^0 p_r, \quad (11)$$

which becomes for a single phase

$$\Omega_g^r/\Omega_g^0 = (1 - v_{eg}^r)/(1 - v_{eg}^0). \quad (12)$$

Combination of Eqs. 8 and 12 results in the overall partition function for a molecule of any given size in any single conformation:[2]

$$\Phi_s^r = \Omega_g^r/\Omega_b^r = 1 - v_{eg}^r, \quad \text{for } v_{eg}^r \le 1;$$
$$\Phi_s^r = \Omega_g^r/\Omega_b^r = 0, \quad \text{for } v_{eg}^r \ge 1, \quad (13)$$

assuming both v_{eb}^0 and $v_{eb}^r = 0$ (see Eqs. 7 and 10). At higher solute concentrations, the self-exclusion volume increases so that $v_{eb}^r \neq 0$ and may increase the partitioning of molecules into the membrane phase (manuscript in preparation).

[2]The implicit assumption in such an analysis is that the molecule can enter the membrane in a conformation/configuration conducive to the space available. When v_e^r approaches v_f^r of the membrane phase, this assumption is true only for very flexible molecules.

Randomly Distributed Volume Exclusion Element

The preceding analysis has assumed that the same volume exclusion element (i.e., size, geometry, and location) exists in a fixed-ordered state within each ensemble volume. These equations are only accurate for a single conformation of the volume exclusion element which is the same in all ensemble volumes so that p is defined for the representative ensemble volume. However, frequently the volume exclusion element(s) of membranes used for chromatography and electrophoresis are not regularly structured and are treated as a randomly oriented and distributed fibrous network. If within any chosen volume both the location and total content of the membrane's volume-excluding element varies randomly, a typical ensemble volume cannot be chosen; however, the total volume still may be divided into equal subunit volumes. The normalized exclusion volume within any subunit volume will vary between 0 and 1, inclusive. However, if the situation is truly random, it must vary in a manner consistent with a binomial distribution of the obstructing species so that the mean volume exclusion of the membrane (v_e^o) equals the summation of the volume exclusion element(s) within each subunit volume (v_{ei}^o) as defined in Eq. 14, especially if the number of subunit volumes (N_v) is quite large. Within each subunit volume the volume exclusion element may be in any one of N_c different distinct conformations. A random volume-excluding element may occupy any coordinate position within the subunit volume so that every single position within each subunit volume must have a finite and equal probability of being occupied. Therefore, the probability (p_c^o) that any single conformation of the volume exclusion element does overlap with a single position occupied by a point molecule within any single subunit volume is simply

$$p_c^o = \sum_{i-1}^{i-N_v} (v_{ei}^o/N_v)/N_c = v_e^o/N_c. \quad (14)$$

Likewise, the same probability for a molecule of finite size relative to a point molecule (p_c^r) is (see derivation of Eq. 10)

$$p_c^r = \Delta v_f^r/(N_c v_f^o) = \Delta v_e^r/(N_c v_f^o) = \frac{v_e^r - v_e^o}{N_c(1 - v_e^o)}. \quad (15)$$

The overall probability ($P_c(n_c)$), that n_c conformations of the volume exclusion element do overlap with a molecule in a fixed position while ($N_c - n_c$) do not, is defined by a binomial distribution that reduces to a Poisson distribution since N_c is large resulting in $p_c \ll 1$ so that

$$P_c(n_c) = \frac{\lambda^{n_c} \exp(-\lambda)}{n_c!}, \quad (16)$$

where $\lambda = N_c p_c^o = v_e^o$ for point molecules and $\lambda = N_c p_c^r = \Delta v_e^r/v_f^o$ for finite size molecules. If n_c equals 0, Eq. 20 reduces to the desired probability of no overlap:

$$P_c^o(0) = \exp(-v_e^o) \quad \text{and} \quad P_c^r(0) = \exp(-\Delta v_e^r/v_f^o). \quad (17)$$

The mean number of accessible states for a molecule is calculated using Eq. 17 in a manner similar to the development of Eqs. 2–13 so that the partition function for any molecule becomes

$$\Phi_s^r = \exp(-v_e^o) \exp[(v_e^o - v_e^r)/(1 - v_e^o)]. \quad (18)$$

Volume Exclusion for Finite-Sized Molecules

The number of accessible states depends strongly on the energy available to that system and increases rapidly with increasing energy. A state is accessible in a thermodynamic sense (which by Eqs. 13 and 18 is dependent on v_e^o and v_e^r) only if the energy of that state is favorable relative to the thermal energy. Hence, a volume is available to a molecule if the interaction energy of the molecule when located in this volume (creating multiple accessible states within this volume) and other surrounding molecules (usually the solvent and the volume-excluding element of the membrane) is favorable. This may be expressed mathematically as a volume integration of the interaction energy (E) within the subunit volume which depends on the position (x, y, z), conformation, and orientation (ψ) of the molecule so that

$$v_f^r = \frac{\sum_{i-1}^{N_f} \int\int\int\int \{\exp[-E_i(x,y,z,\psi)/kT]/N_f\} d\psi\, dx\, dy\, dz}{\int\int\int \exp(-E^*/kT)\, dx\, dy\, dz} = 1 - v_e^r, \quad (19)$$

where k is the Boltzmann constant, T is temperature, and the center of the partitioning molecule is placed at coordinate positions (x, y, z) and E is evaluated over all positions (within the volume) of the molecule for any single conformation i of N_f possible conformations. The energy term E consists of the combined intermolecular and intramolecular interaction energies of the solvent, volume-excluding elements, and permeating molecules. The superscipt * indicates a logical reference state which in this case is a state without any permeating molecules. Therefore, v_e^r becomes the mean effective volume excluded from the molecule within the membrane phase. For only steric interactions, E_i equals zero whenever the molecule and the membrane's volume-excluding element do not overlap and is infinite when they do. E^* equals 0 when only steric interactions are considered, especially if the solvent is treated as a continuum.

As E within the volume integration increases, v_e^r

increases and v_f^r decreases until $v_e^r = 1$ and $v_f^r = 0$ when E approaches infinity (relative to kT). For example, when solute and membrane are similarly charged, electrostatic repulsion increases E as the membrane and the molecule approach each other so that integration of Eq. 19 predicts the intuitively obvious result that v_e^r increases. If E is negative as in the case of adsorption to the membrane, v_f^r may become greater than 1 so that v_e^r is negative and Φ is greater than 1.

Specific Geometry of the Molecule and Membrane

The analysis up to this point has been kept very general with few inherent assumptions and details about the membrane phase. These general results may be applied to any particular membrane system when v_e^r is defined by the geometry of both the permeating molecule and the volume exclusion element of the membrane phase. In this section specific partition functions are developed for several different membrane and molecular geometries from the generalized expressions given by Eq. 13 or 18 combined with Eq. 23 when only steric interactions are considered. The specific expressions are compared to past results derived using a different approach.

For rigid molecules of arbitrary shape, Eq. 19 may be simplified considerably if only steric interactions are considered:

$$v_f^r = \int\int\int \exp\left[-E(x, y, z)/kT\right] dx\, dy\, dz \Big/ \int\int\int dx\, dy\, dz = 1 - v_e^r. \quad (20)$$

This integral can be solved for any arbitrary shape of both the volume-excluding element and the solute. For a simple assembly of rodlike fibers of radius r_f and of length per unit volume L, Eq. 20 defines a volume exclusion of radius r_m:

$$v_e^r = \Pi r_m^2 L = v_e^o (r_m/r_f)^2 \rightarrow v_e^o (1 + r_p/r_f)^2, \quad (21)$$

where

$$r_m = \int r\, d\psi \Big/ \int d\psi, \quad (22)$$

where r is the distance of closest approach between the center of the molecule and the volume-excluding element, which in this case is a cylindrical fiber, measured over all possible orientations. One may envision this process as rolling the molecule over the surface of the fiber and measuring the distance between the centers of the molecule and fiber. For spherical molecules (radius = r_p), r_m is simply r_p plus r_f since both are constant for all possible orientations (ignoring fiber end effects). For a solute molecule shaped like a capsule consisting of a hemisphere of radius r_r capping each end of a cylinder of radius r_r and half-length r_L, one gets:[3]

$$r_m = (2/\pi)\big((r_f + r_r)\{\theta - \ln[\tan(\theta/2)]\} + r_L(\cos\theta + \sin\theta - 1)\big), \quad (23)$$

where $\theta = \arctan[(r_f + r_r)/r_L]$.

Regardless of the shape of the molecule or the volume-excluding element, r_m can be evaluated, if need be by numerically summating the distance over many orientations (with accuracy increasing as the number of tested orientations increases). Since the three-dimensional structures of many macromolecules have been determined by x-ray crystallography and are available in the Protein Data Bank, Eqs. 21 and 22 may be used with the specific coordinate positions of atoms within the molecule to assess graphically or calculate numerically r_m, v_e^r, and the mean radius of the molecule (22). With v_e^r evaluated, Eq. 13 or 18 may be used to calculate the partition function for any arbitrarily shaped molecule or volume-excluding element(s).[4]

Cylindrical Fiber Matrix Model. For a membrane with a fixed uniform meshwork of cylindrical fibers, Eq. 13 combined with Eq. 21 becomes for any molecule of arbitrary shape

$$\Phi = 1 - v_e^o(r_m/r_f)^2, \quad r_m \le r_f v_e^{o-1/2}: \Phi = 0, \quad r_m \ge r_f v_e^{o-1/2} \quad (24)$$

and for a randomly oriented and distributed meshwork of fibers, Eq. 18 becomes

$$\Phi = \exp(-v_e^o) \exp\{v_e^o[1-(r_m/r_f)^2]/(1-v_e^o)\}, \quad (25)$$

---

[3] For more complex geometries such as prolate ellipsoids of revolution and oblate ellipsoids, an analytical approximation for r_m is possible using the solution of Giddings et al. (16) (add $2r_f$ to their analytical expression for the mean external length of the molecule and divide this sum by 2 to get r_m). However, this expression tends to overestimate r_m since the site of tangential intersection of the molecule and fiber is not necessarily on the central axis (fiber center to molecule center). Exact analytical solutions for r_m are nontrivial. Another approach may be to evaluate v_e^r utilizing the area projection method of Giddings et al. (16) (multiply the fiber length per unit volume by the mean area of the fiber interacting with the molecule projected over all directions in space). Molecular projection areas are given for several interesting molecular geometries (16).

[4] Frequently the volume-excluding element is not distributed uniformly or randomly but is distributed either continuously or discretely over a range of values. For example, the radii of the pores of a membrane may vary. Also, the exclusion element may consist of different geometric forms. If the distribution of volume exclusion elements is known and the volume-excluding elements are independent of each other, then for rigid molecules and for steric interactions only Eq. 20 reduces to

$$v_e^r = \Sigma\, v_{ei}^r \text{ or } \int v_{ei}^r\, dr, \quad (F1)$$

where i represents the different exclusion volumes. If the assembly of volume excluding elements is continuous in its distribution then the integral term should be used; otherwise, for a discrete, noncontinuous distribution the summation term suffices.

where r_m is defined by Eq. 22 (equals $r_f + r_p$ for spherical molecules), v_e^o may be defined either by $\Pi r_f^2 L$ (L is fiber length per unit volume) if independent structural details are available or $\rho_s g$ where ρ_s is the effective specific volume of the gel and g is the concentration of the gel (wt/vol). This result clearly differs from the results of OG theory (see Eq. B2).

Other Membrane Geometries. Eqs. 13 and 18 are solved for cylindrical pore and planar membrane models. Since many of these expressions agree with those of Giddings et al. (16), they are presented in Appendix A. Expressions for Φ for membranes with continuous or discrete distributions of radii (i.e., pore or fiber radii) are also included in Appendix A.

RESULTS

This analysis first proves in a general manner without specifying the geometry of the membrane's volume-excluding element that for a point molecule the relative number of accessible states between two volumes in equilibrium is either directly proportional to (ordered membrane structure) or exponentially dependent on (random membrane structure) the volume available to that molecule within each state. Then, the partition behavior of any molecule is calculated from the accessibility-state ratio for finite size molecules relative to point molecules which is dependent on the relative change in free or exclusion volume for the two molecules. The analysis is performed for both uniform (Eq. 13) and random (Eq. 18) volume exclusion elements. Finally, the partition function specifically is calculated using various geometries for the permeating molecule and the volume exclusion element and compared with past analyses.

In this section, first the general effects of the membrane volume exclusion are discussed briefly without specifying the geometry of the permeating molecule or the volume-excluding element of the membrane. The partition function for a random fiber matrix is applied to gel chromatography and electrophoresis (see Appendix B). The model is tested using data derived from experiments on molecular mobility during gel electrophoresis and on molecular partition behavior during size exclusion chromatography. An expression predicting the minimum exclusion radius of molecules totally excluded from a random fiber matrix is tested and compared with available experimental data. Finally, the predictions of this analysis and the OG theory are directly compared to each other in terms of the partition function and retardation coefficient.

General Volume Exclusion Effects

Fig. 1 shows the effect of the membrane volume exclusion (v_e^o) on the steric partition function (Φ), the relative mobility of the molecule (μ/μ_o, $\log(\mu/\mu_o)$), and both the partition function ratio (Φ_{OG}/Φ) and mobility ratio (μ_{OG}/μ) as predicted by the Ogston/Giddings models (OG) with their extensions and by this new theory when the relative volume exclusion for a molecule (v_e^r/v_e^o) is kept constant (i.e., molecular radius and fiber radius). To make this comparison possible, the OG theory is generalized so that $\Phi = \exp(-v_e^r)$. As the membrane volume exclusion increases, the steric partition function of any sized molecule decreases, the extent of which depends on the total volume excluded from that molecule (v_e^r). The partition function for a point molecule where v_e^r equals v_e^o decreases slowly with increasing v_e^o. However, as v_e^r/v_e^o increases, the partition function decreases very rapidly. As shown in Fig. 1 the discrepancy between the predictions of this theory and the OG theory increases significantly with increasing v_e^o and v_e^r. The OG theory predicts a partition function always greater than or equal to the present theory. When v_e^o equals v_e^r the predictions of both theories are the same; however, very large differences may become apparent as the membrane volume exclusion and/or the molecular size increase. Intuitively, it is obvious that as the volume-excluding element occupies all of the space within a volume ($v_e^o \rightarrow 1$), Φ must approach 0. All of the new expressions for the steric partition function (Eqs. 13, 18, 24, and 25)

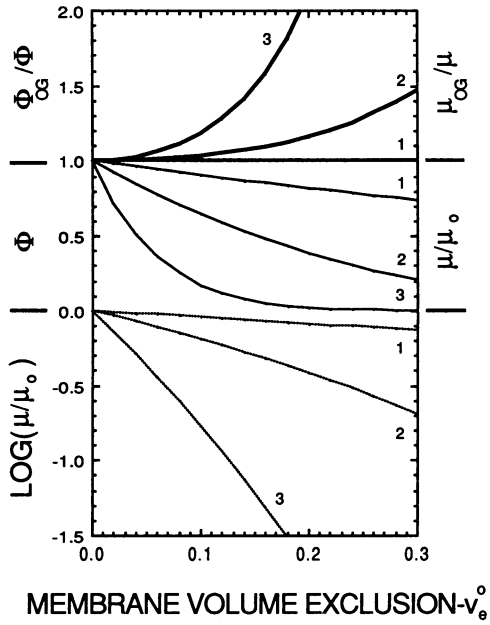

FIGURE 1 The effect of the membrane volume exclusion (v_e^o and v_e^r) on the steric partition function (Φ), the relative mobility of the molecule (μ/μ_o, $\log(\mu/\mu_o)$), and both the partition function ratio (Φ_{OG}/Φ) and mobility ratio (μ_{OG}/μ) as predicted by the OG theory and this new theory. The thin solid curves represent Φ and μ/μ_o. The dotted curves represent $\log(\mu/\mu_o)$, and the thick solid curves signify both Φ_{OG}/Φ and μ_{OG}/μ. Φ is evaluated using Eq. 18 and is extended to predict molecular mobility via Eq. B1 (see Appendix B). For each curve the relative volume exclusion for a molecule ($f = v_e^r/v_e^o$) is kept constant (curve *1*, $f = 1$; curve *2*, $f = 4$; curve *3*, $f = 16$). In terms of a cylindrical model of a fibrous gel, f equals 1 if the equivalent spherical particle radius is 0; $f = 4$ if $r_p/r_f = 1$; and $f = 16$ if $r_p/r_f = 3$.

predict Φ equals 0 for all finite-sized molecules if v_e^o is 1. However, the OG expression (Eq. B2) clearly does not.

Since the mobility ratio is equal to the partition function (Eq. B1), it has the same dependency on v_e^o and v_e^r (see Fig. 1). The difference in the predictions of the two theories is also the same. The plot of log (μ/μ_o) vs. v_e^o shown in Fig. 1 is essentially a Ferguson plot. The logarithm of the mobility of a point molecule (where v_e^r equals v_e^o) decreases slowly and almost linearly with increasing v_e^o. However, as v_e^r/v_e^o increases, the logarithm of the mobility ratio decreases more rapidly in a curvilinear manner. This nonlinearity may be interpreted as increasing the retardation coefficient as v_e^r/v_e^o increases (see later results).

Comparison to Gel Electrophoresis Data

As a test of this new analysis, the predicted Ferguson plots as expressed by Eq. 25 combined with Eqs. B1 and B4 were compared to the available experimental data of the electrophoretic mobility of various molecules through agarose gels (see Figs. 2–4). These figures show the nonlinear effects of gel concentration/percentage of agarose on the electrophoretic mobility of molecules. The logarithm of the mobility ratio (μ/μ_o – mobility of molecules in gels/mobility assessed at a gel concentration of 0) equals 1 as the volume exclusion approaches 0, as expected. The experimental data indicate that the nonlinearity increases with membrane volume exclusion and molecular size, in agreement with the theoretical results presented in Figs. 1–4.

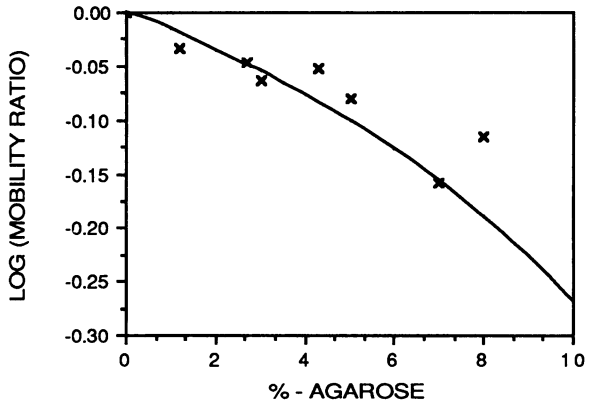

FIGURE 2 Ferguson plot of the mobility of ovalbumin during agarose electrophoresis. The experimental data points were graciously provided by Dr. D. Tietz and Dr. A. Chrambach as published previously (20, 21). The solid curve represents an extension of Eq. 18 (see Appendix B) with all variables defined by available experimental data (see text). A hydrodynamic radius of 2.76 nm (as defined by the standard Stokes–Einstein relation to diffusion) was used for the molecular radius (r_p). An effective specific volume for the agarose of 1.0 was used, a value justified by the high water content of the fibers (26, 27). The data of Waki et al. (23) were used to estimate the fiber radius of the agarose gels with linear interpolation between the available data points (see Fig. 5). The fiber radius varied from 5.0 nm at 0.25% to 2.0 nm at 10% agarose.

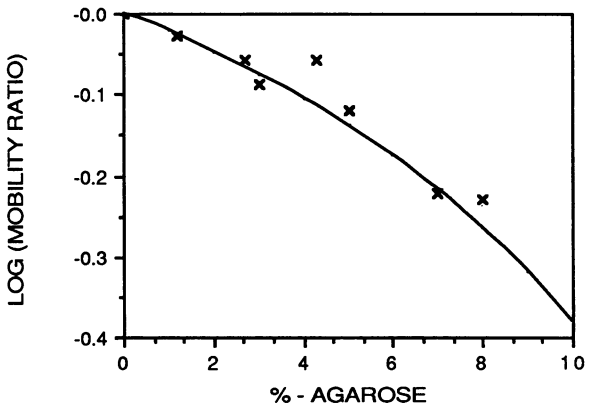

FIGURE 3 Ferguson plot of the mobility of bovine albumin during agarose electrophoresis. The hydrodynamic radius is 3.64 nm. All other parameters defined in legend to Fig. 2.

Recent electron microscopic examination of agarose gels indicates that the agarose fiber radius should not be considered a constant over the range of gel concentrations tested (20). As shown graphically in Fig. 5 from the work of Waki et al. (23), the fiber radius clearly decreases as the gel concentration increases. Therefore, the fiber radius used in modeling these data was estimated as a function of gel concentration by simple linear interpolation between the available data points (solid line in Fig. 5). The Ferguson plots given in Figs. 2–4 are developed using this expression for the fiber radius so that all variables of the model are known. With all model parameters defined by available experimental data, the theoretical expression provides an excellent nonlinear fit of the Ferguson plot of these data for all three molecules tested.

Comparison to Gel Chromatography Data

The model developed by Laurent and Killander (2) is used to extend the new expression for the partition function to

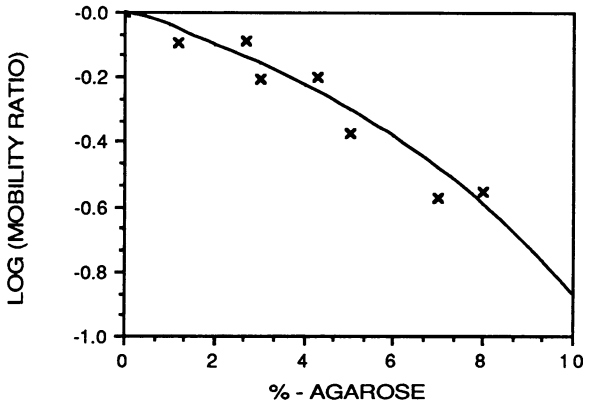

FIGURE 4 Ferguson plot of the mobility of phosphorylase b during agarose electrophoresis. The hydrodynamic radius is 6.52 nm. All other parameters defined in legend to Fig. 2.

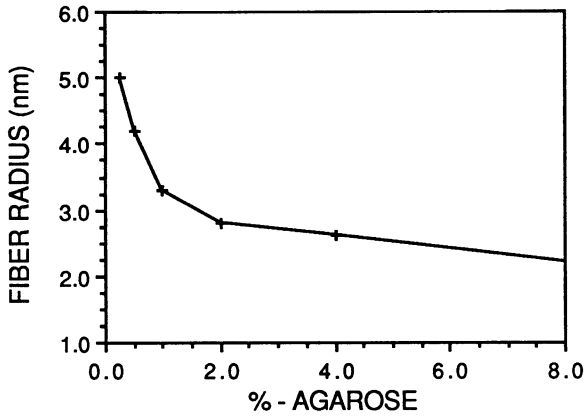

FIGURE 5 Dependence of the agarose fiber radius on gel concentration. The + symbol represents the fiber radius determined by Waki et al. (23) who examined agarose gels using electron microscopy. The solid line represents linear interpolation between data points and was the function used to estimate the fiber radius at any given gel concentration.

size-exclusion chromatography (see Appendix B, Eq. B5). As shown in Fig. 6, Eqs. 18 and B5 fit experimental data on the partitioning of many different macromolecules during gel chromatography through various Sephadex columns. All parameters within the model are defined except for the membrane volume exclusion which apparently varies with different batches of Sephadex so that only a range of values is available. Therefore, the model was tested by numerical optimizing v_e^0 as a single unknown variable utilizing a finite difference Levenberg-Marquardt algorithm to minimize the sum of the squares of the difference (24). The v_e^0 resulting in the best fit agrees well with the range of v_e^0 (calculated from the bed volume to weight dry Sephadex

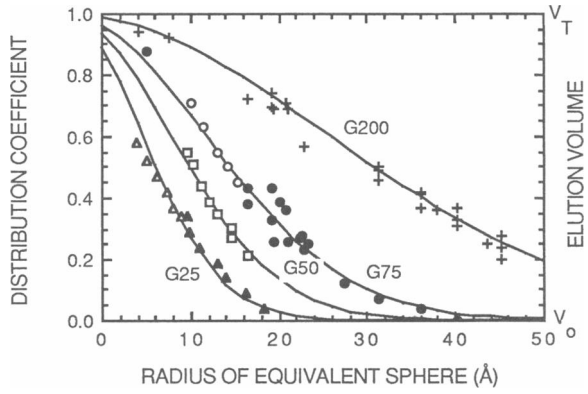

FIGURE 6 Size selectivity curves for Sephadex gel chromatography of various macromolecules. Experimental data from chromatography through G200, G75, G50, and G25 Sephadex columns using various macromolecules. The data points are compiled from several studies as tabulated by Laurent and Killander (2). The Δ and O symbols represent various dextran molecules, whole Δ and O are degradation products of cellulose. The other symbols represent various other molecules including globular proteins. The molecular hydrodynamic radius was used as calculated and tabulated previously (2). The specific volume of dextran is 0.61 (2). The fiber radius used was 4.5 Å, a value consistent with the molecular structure of dextran.

ratio) given by Pharmacia Fine Chemicals (Piscataway, NJ) for their Sephadex columns.

Prediction of Minimum Exclusion Radius

To test this model further with available experimental data, an expression is derived from the general partition function (Eq. 18) predicting the minimum radius of a spherical molecule that cannot enter a random fiber matrix gel by solving for r_p:

$$r_{pL} = \left(\sqrt{\frac{(v_e^0 - 1)(\ln \Phi_L + v_e^0) + v_e^0}{v_e^0}} - 1 \right) r_f, \quad (26)$$

where r_{pL} is the limiting or minimum particle radius that cannot enter the gel (the minimum exclusion radius) and Φ_L is the desired minimum partition value (a very small nonzero value).

Fig. 7 shows excellent theoretical agreement with the data of Serwer and Hayes (25) who studied the exclusion of spheres by agarose gels and its dependence on sphere radius and gel concentration. The predictive error percentage is <20% for all points with an average absolute value of 7.84%. Values of r_{pL} decrease as a nonlinear function of gel concentration. This expression is the first nonempirical expression based on steric exclusion theory that adequately predicts the minimum exclusion radius of a molecule. Previously, only empirical linear expressions were available for predicting this exclusion radius (25).

Direct Comparison to the OG Theory and its Extensions

Comparison of the analytical solutions for the steric partition functions developed by Ogston (15) and Giddings et al. (16) (the OG theory) with the results of this analysis indicate exactly the same expressions for plane (Eqs. A4 and A5) and cylindrical pore (Eq. A1) membrane models; however, differences may be quite significant for mem-

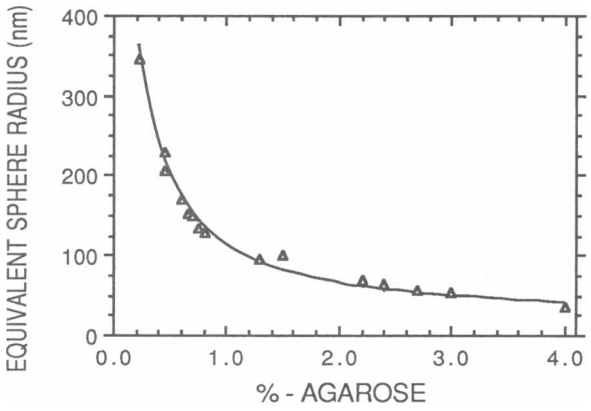

FIGURE 7 Minimum exclusion radius for a molecule in an agarose gel. The △ represent the data of Serwer and Hayes (25). The solid line is defined by Eq. 26 with all model parameters defined experimentally. The model was numerically optimized to the experimental data since Φ_L (effective zero partition value) is arbitrary ($\Phi_L = 7.5 \times 10^{-5}$).

branes consisting of a random assembly of rodlike fibers (Eqs. 25 and B2). Even in this case, it is clear that this analysis predicts the same trends predicted by the OG expression (with quantitative differences) for changes of partition parameters such as r_f, g, r_p, etc. Rather than repeat the graphical results showing the effect of these various parameters on the partition function (15, 16), the predictions of the two approaches are compared directly. The general rule evident from this comparison is that they agree when the volume exclusion is very small.

The two expressions (Eqs. 25 and B2) for the partition function are compared analytically in Appendix C (Eq. C1) and graphically in Fig. 8. The percentage that the new partition function (Φ) is reduced when compared to the OG expression (Φ_{OG}) is a function of the r_p to r_f ratio for different gel concentrations or volume exclusions. Φ_{OG} is always $\geq \Phi$. The percent difference approaches zero as v_e^o, ρ_s, g, and/or r_p/r_f approach zero. As the values of these parameters become greater than 0, the disparity between the two expressions increases significantly. For any given g, as r_p and v_e^r increases, the percent reduction becomes greater until a plateau of 100% relative reduction is reached. This reduction is more pronounced at any given r_p/r_f ratio as g and its dependent parameters (i.e., v_e^o and v_e^r) increase. As g increases, the new expression for the partition function approaches 0 much more rapidly than the OG expression so that the relative error reaches a maximum of 100% at smaller r_p/r_f values.

The current theory of the mobility of molecules during gel electrophoresis is based on the OG model and predicts a constant retardation coefficient (slope of a Ferguson plot) for any particle transported through a random fiber matrix (3,4, and Appendix B). However, as shown directly by Eq. B6 and by the theoretical and experimental data in Figs. 2–4, the retardation coefficient may not be constant. The new expression for the partition behavior of molecules in random fibrous gels yields an expression for the retardation coefficient (Eq. B6) that varies with gel concentration. When compared to the OG expression, the fractional difference between the two expressions is defined analytically by Eqs. C2 and C3. Fig. 8 shows the percentage difference of the two expressions. The new expression is always greater than or equal to the OG expression. When v_e^o is very small ($v_e^o \rightarrow 0$), the two analytical expressions agree. However, as v_e^o increases, the discrepancy increases rapidly and becomes very large with the limiting difference given by Eq. C3. The discrepancy increases as either r_p/r_f, v_e^o, v_e^r, or g increases (the error becomes negligible as the magnitude of any of these parameters approaches zero). As shown in Fig. 9, the percentage increase approaches a plateau rapidly as a function of $r_p r_f$. When the particle and fiber radius are equal, a maximum difference is reached; therefore, this difference may be significant even at low r_p/r_f values.

DISCUSSION

This analysis in its most general form (Eqs. 13 and 18) provides a derivation of the partition function and its extensions for any geometry of the volume-excluding element and permeating molecule (see Fig. 1). Specific mathematical expressions are derived for molecules of arbitrary shape partitioning within membranes containing an assembly of cylindrical pores, planes, and rodlike fibers (with uniform, random, or nonrandom distributions). These expressions agree with those of Giddings et al. (16) for the simpler membrane geometries including networks of cylindrical pores (Eq. A1), planes (Eqs. A4 and A5), and even uniform fibers (Eq. 24). However, for a membrane consisting of an assembly of randomly distributed and oriented fibers, the expression differs significantly (compared Eqs. 25 and B2). Therefore, the random fiber matrix model was tested using data from agarose gel electrophoresis analyzed by Ferguson plots (see Figs. 2–4). With all variables within the model defined experimental-

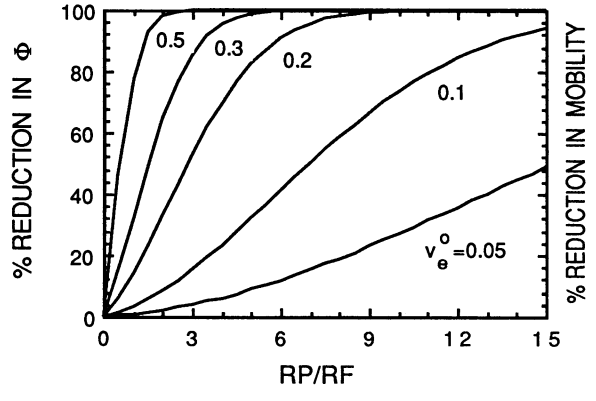

FIGURE 8 Comparison of the partition function of this theory and the OG theory. The percent reduction in the partition function as calculated by 100% $(\Phi - \Phi_{OG})/\Phi_{OG}$ (Eq. C1) is plotted as function of the particle to fiber radius for various gel concentrations (g). For an effective specific volume of 1.0, $g = v_e^o$.

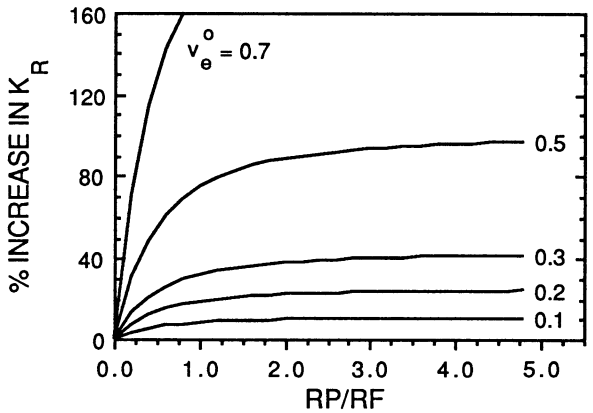

FIGURE 9 Comparison of the retardation coefficient predicted by this theory and the OG theory. The percent increase as calculated by 100% $(K_R - K_{RO})/K_{RO}$ (Eqs. C2 and C3) is plotted as a function of r_p/r_f for various gel percentages. Other parameters as in Fig. 8.

ly, it agrees well with the data and predicts the nonlinear behavior of the Ferguson plots. In keeping with experimental observations (16–21), this analysis predicts that the nonlinearity of Ferguson plots increases as the size of the molecule or particle increases. The model also shows excellent agreement with size selectivity curves for gel chromatography (see Fig. 6). In addition, an expression for the minimum exclusion radius of a molecule to a gel is derived and shown to agree well with recent experimental data (see Fig. 7).

A direct comparison to the standard OG-based theories shows virtual agreement between these theories only at very low volume exclusions. Differences in the prediction of both partition functions and retardation coefficients may be very significant and increase rapidly with increasing volume exclusion and molecular size (see Figs. 1, 8, and 9). Φ_{OG} is always $\geq\Phi$. For any molecule of arbitrary shape, the crucial parameters describing partition behavior in this new model clearly are v_e^o (membrane volume − volume excluded to a point molecule) and v_e^r (volume excluded to a finite-sized molecule). Without specifying the geometry of the membrane's volume-excluding element, this analysis proves that for a point molecule the relative number of accessible states between two volumes in equilibrium is dependent on the volume available to that molecule within each state. Then, the partition behavior of any molecule is calculated from the accessibility-state ratio for finite size molecules relative to point molecules, which is dependent on the relative change in free or exclusion volume for the two molecules. However, in the Giddings et al. model (16), they assume that partitioning is dependent only on the volume available to the molecule.

As in the OG analyses, the final analytical expression for molecular partitioning in a random fiber matrix assumes that the fiber network–particle interaction is negligible, other than the steric, space-occupying effects. Obviously, particle–fiber interactions do exist, may be significant and may vary depending on the gel type, the environmental conditions (i.e., ionic strength of the solution, pH), and the permeating molecule itself (28). Since most polyelectrolytes contain hydrophilic, ionic, and hydrophobic groups, electrostatic and van der Waal forces along with hydration, hydrogen bonding, and hydrophobic considerations can affect particle–fiber interactions, especially near the fiber surface. It is intuitively evident that the sum of the interaction forces may result in attraction or repulsion of the particle in the volume near the fiber, thereby changing the partition behavior of the molecule within this volume. This concept is expressed mathematically in Eq. 19. Each relative position of the particle and the volume exclusion element may not have the same free energy and therefore the same probability of existence. If the forces are significant, the calculated v_e^r, assuming accurate knowledge of v_e^o, will only represent an apparent mean effective volume exclusion for the molecule. If these forces are repulsive in nature so that the interaction energy is positive, Eq. 19 predicts that v_e^r will be larger than its true steric value, resulting in a lower partition function. If particles are attracted towards or bind the volume-excluding element, the observed v_e^r may be smaller than its true value to the extent that the observed Φ may even become positive.[5]

This analysis provides a logical framework for evaluating important factors in partition behavior such as electrostatics (work in progress) and molecular concentration effects (manuscript in preparation) from both experimental and theoretical perspectives. The general expressions for the partition function (Eqs. 13 and 18) provide a simple approach to defining the partition behavior of molecules in a porous membrane. These two equations only require two fundamental parameters to fully describe the partitioning of solutes in membranes: v_e^o and v_e^r. Since v_e^o is well defined for many membrane systems,[6] v_e^r is the only unknown variable in Eqs. 13 and 18 so that a mean effective value can be evaluated (using rigorous statistical methods already developed [4]) from elution volume data, size selectivity curves, Ferguson plots, or partition data. Under ideal conditions, v_e^r will increase in proportion to v_e^o or g; however, in reality v_e^r will be affected by membrane–molecule interactions[7] or even changes in the geometry of the volume-excluding element that may occur with gel

[5]In size-exclusion chromatography, the interaction of anionic polyelectrolyte with anionic chromatographic packing frequently results in peaks eluting earlier than expected (lower apparent K_{av}, see Eq. B5) so that the molecular weight is overestimated. For cationic polyelectrolytes, depending on the extent of adsorption, K_{av} may be quite large so that elution volumes are very large, sometimes greater than the bed volume (28). If r_p and v_e^o are kept constant, v_e^r and therefore K_{av} will appear to vary with environmental factors such as ionic strength, pH, ions, and solvent used. The effect of charge on partition behavior could be assessed by using several molecules of different charge but very similar flexibility and hydrodynamic radius (possibly by different degrees of charge modification of a single protein).

[6]Several different methodologies can be used to evaluate confidently v_e^o. The v_e^o may be estimated by $\rho_s g$ or more rigorously from structural studies (i.e., x-ray diffraction, electron microscopy). It also may be defined functionally by using a series of very small probes (relative to the scaling factor of the volume excluding element, i.e., r_f for fibrous gels, r_p for cylindrical pores) which do not interact with the membrane (i.e., without charge). Such probe molecules may be treated as a point molecules so that v_e^o may be calculated easily from a simplified Eq. 13 or 18 ($v_e^r = v_e^o$). Several small probes of similar size should be tested, all resulting in the same v_e^o if no membrane–molecule interactions exist.

[7]Many other factors may effect the observed effective v_e^r. Obviously, any changes in the scaling terms defining the membrane exclusion volume (i.e., r_r and L for fibrous gels) with gel concentration or environmental conditions will alter v_e^r. The degree of hydration which may change both with gel concentration and environmental conditions may significantly alter v_e^r. Adsorption of other molecules to the membrane could increase v_e^r. In addition, fluid flow may alter hydrodynamically the preferred orientation of the molecule relative to the membrane so that the apparent v_e^r changes. All of these considerations are important in truly understanding the partition behavior of molecules in porous membranes and can be systematically evaluated using Eqs. 13 and 18 with one unknown variable v_e^r.

concentration (20, 21, 27), pH, or ionic conditions (28). Ideally several molecular probes of similar size are needed to systematically evaluate possible interactions between the permeating molecule and the excluding membrane. As discussed earlier, if a probe interacts with the volume exclusion element, the apparent v_e^r will differ from the other noninteracting test probes. Using this type of approach any membrane partition system can be evaluated so that any observed changes in v_e^r will be the first indications of more complex interactions necessitating both very systematic functional and structural characterization of v_e^o and v_e^r. By using v_e^r as the dependent variable, the effects on molecular partition behavior, gel chromatography, and gel electrophoresis of important factors such as charge, degree of hydration, degree of gel cross-linking, pH, and ion concentration can be tested and analyzed systematically.

APPENDIX

A. Specific Membrane Geometries

Cylindrical Pore Membrane Model. For a membrane with cylindrical pores of uniform radius r_c and for spherical molecules of radius r_p, Eq. 13 becomes

$$\Phi_s^r = v_c^o(1 - \beta)^2 = v_f^r, \quad \beta \le 1; \quad \Phi = 0, \quad \beta \ge 1, \qquad \text{(A1)}$$

where $\beta = r_p/r_c$ and v_c^o is the volume of the cylindrical pore(s) per unit total volume and equals $n_c \Pi r_c^2 t$ with n_c being the number of pores per unit total volume, with radius r_c and t being the membrane thickness. Eq. A1 agrees with past results for this simple membrane geometry (16). If the volume exclusion of this membrane is not uniform but is random, Eq. 18 is used to get

$$\Phi_s^r = \exp(v_c^o - 1)\exp(\beta^2 - 2\beta). \qquad \text{(A2)}$$

If the distribution of pore sizes is known, Eq. F1 (see footnote 4) results in

$$\Phi = \sum_{r=r_{min}}^{\infty} v_c^o(r)(1 - r_p/r)^2 \text{ or } \int_{r_{min}}^{\infty} v_c^o(r)(1 - r_p/r)^2\, dr, \qquad \text{(A3)}$$

where r_{min} is the minimum pore radius and $v_c^o(r)$ equals $n_c \Pi r^2 t$ with n_c being the number of pores with radius r per unit total volume. For an assembly of cylindrical pores with a continuous distribution of radii, the integral term should be used. Otherwise for pores with a discrete distribution of radii the summation term is appropriate.

Planar Membrane Model. For a regularly ordered network of planes, Eq. 13 ($v_e^o = 0$; $v_e^r = sr_m$) results in

$$\Phi_s^r = 1 - sr_m, \quad r_m \le 1/s; \quad \Phi_s^r = 0, \quad r_m \ge 1/s, \qquad \text{(A4)}$$

where s is the mean surface area of the planes per unit volume and r_m is defined by Eq. 22 and in this case represents the mean external radius of the molecule which for spherical molecules equals r_s. For an isotropic network of random planes, one gets

$$\Phi_s^r = \exp(-sr_m). \qquad \text{(A5)}$$

Both Eqs. A4 and A5 agree with past results (16) with r_m being the crucial dimension.

Fiber Matrix Model with Nonuniform Distribution of Fiber Radii. For a regularly structured network of fibers with a discrete distribution of radii (see Eq. F1):

$$\Phi_s^r = 1 - \sum_{r=r_{min}}^{r_{max}} v_e^o(r)(r_m/r)^2 \qquad \text{(A6)}$$

and for a randomly structured fiber matrix with a distribution of fiber radii:

$$\Phi_s^r = \exp\left[\sum_{r=r_{min}}^{r_{max}} v_e^o(r)\right]\exp\left\{\sum_{r=r_{min}}^{r_{max}} v_e^o(r)[1 - (r_m/r)^2]\right\}, \qquad \text{(A7)}$$

where v_e^o is defined by r and each summation is over the range of fiber radii (minimum to maximum radius). If the distribution of radii is continuous, an integral solution may replace the summation solution.

B. Application to Gel Filtration and Electrophoresis

Original Functions from the OG Theory and its Extensions. To describe the effects to gel sieving on the mobility of a particle through a gel (μ), the reduction factor by which particles are slowed by sieving during gel filtration or electrophoresis is usually assumed to be the probability that a randomly positioned and oriented particle intersects with the volume exclusion element of the membrane (2–4). This factor is equivalent to the partition function (3, 4) so that

$$\mu = \mu_o \Phi_s^r = \mu_o \exp(-K_R g), \qquad \text{(B1)}$$

where μ_o represents the free electrophoretic mobility of particle at 0% gel concentration and the retardation coefficient (K_R) is either empirically derived or described by an extension of the OG theory, which defines Φ as

$$\Phi_s^r = \exp[-v_e^o(1 + r_p/r_f)^2] = \exp[-\Pi L(r_f^2 + r_p^2)] \qquad \text{(B2)}$$

so that

$$K_R = v_e^o(1 + r_p/r_f)^2/g = \Pi L(r_f^2 + r_p^2)/g = \rho_s(1 + r_p/r_f)^2. \qquad \text{(B3)}$$

Ferguson plots classically define this coefficient which describes the restriction of the electrophoretic mobility of the molecule via the expression

$$\log(\mu_p) = \log(\mu_o) - K_R g, \qquad \text{(B4)}$$

where in this case $K_R = -\ln(\Phi)/[g \ln(10)]$. This theory predicts a simple linear relation between the log (mobility ratio) and the gel concentration for all gel concentrations and types of fibrous gels. The retardation coefficient is constant.

The separation mechanism of size-exclusion chromatography is based on the differential permeation of molecules into and out of porous beads packing into a chromatographic column. Laurent and Killander applied the Ogston model to gel filtration by assuming that the filtration coefficient K_{av} equals to the partition function and is related to the elution volume (V_{el}) by the equation

$$K_{av} = \Phi_s^r = \frac{V_{el} - V_0}{V_T - V_0}, \qquad \text{(B5)}$$

where V_0 is the void volume of the gel column and V_T is the total volume.

Functions from the Present Theory. The partition expression given by Eq. 18 defines molecular mobility in gel electrophoresis via

Eq. B1, elution volumes in gel chromatography via Eq. B5, and the retardation coefficient as

$$K_R = v_e^o[(1+r_p/r_f)^2 - v_e^o]/[g(1-v_e^o)], \quad \text{(B6)}$$

which can be used with Eq. B4 (divide Eq. B6 by ln (10)) to define Ferguson plots.

C. Comparison to OG Theory

The relative change in the partition functions derived by this new theory (Eq. 25) and the OG theory (Eq. B2) is simply

$$\frac{\Phi - \Phi_{OG}}{\Phi_{OG}} = \exp \frac{(v_e^o)^2(2f+f^2)}{1-v_e^o}, \quad \text{(C1)}$$

where $f = r_p/r_f$. The relative change in the K_R predicted by both theories is (Eqs. B3 and B6)

$$\frac{K_R - K_{RO}}{K_{RO}} = \frac{v_e^o[1-(1+a/r_f)^2]}{(v_e^o-1)(1+a/r_f)^2}. \quad \text{(C2)}$$

When the r_p/r_f is $\gg 1$, then Eq. C2 reduces to

$$(K_R - K_{RO})/K_{RO} = v_e^o/(1 - v_e^o). \quad \text{(C3)}$$

This work has been supported in part by National Heart, Lung, and Blood Institute grant HL-17080 and by a gift from R.J.R. Nabisco, Inc.

Received for publication 23 May 1988 and in final form 15 August 1988.

REFERENCES

1. Tiselius, A., J. Porath, and P. Albertsson. 1963. Separation and fractionation of macromolecules and particles. *Science (Wash. DC).* 141:13–20.
2. Laurent, T. C., and J. Killander. 1964. A theory of gel filtration and its experimental verification. *J. Chromatogr.* 14:317–330.
3. Rodbard, D., and A. Chrambach. 1970. Unified theory for gel electrophoresis and gel filtration. *Proc. Natl. Acad. Sci. USA.* 65:970–977.
4. Rodbard, D., and A. Chrambach. 1971. Estimation of molecular radius, free mobility, and valence using polyacrylamide gel electrophoresis. *Anal. Biochem.* 40:95–134.
5. Laurent, T. C. 1964. The interaction between polysaccharides and other molecules. *Biochem. J.* 93:106–112.
6. Solomon, A. K. 1968. Characterization of biological membranes by equivalent pores. *J. Gen. Physiol.* 51:335–364.
7. Schnitzer, J. E. 1986. A mathematical analysis of lipid charge effects on electrophoresis, hydrophobic ion adsorption, and membrane conductance. *Biophys. J.* 49:515a. (Abstr.)
8. Schnitzer, J. E., and C. C. Lambrakis. 1988. Multi-dimensional numerical solutions for electrostatic interaction of charged molecules with lipid membranes and ion channels. *Biophys. J.* 53:399a. (Abstr.)
9. Mastro, A. M., M. A. Babich, W. D. Taylor, and A. D. Keith. 1984. Diffusion of a small molecule in the cytoplasm of mammalian cells. *Proc. Natl. Acad. Sci. USA.* 81:3414–3418.
10. Swanson J. A., and P. L. McNeil. 1987. Nuclear reassembly excludes large macromolecules. *Science (Wash. DC).* 238:548–550.
11. Curry, F. E., and C. C. Michel. 1980. A fiber matrix model of capillary permeability. *Microvasc. Res.* 20:96–99.
12. Schnitzer, J. E., and W. W. Carley. 1986. Electrostatic and steric partition function of the endothelial glycocalyx. *Fed. Proc.* 45:1152.
13. Polefka, T. G., R. A. Garrick, W. R. Redwood, N. I. Swislocki, and F. P. Chinard. 1984. Solute-excluded volumes near the Novikoff cell surface. *Am. J. Physiol.* 247:C350–C356.
14. Schnitzer, J. E. 1988. Glycocalyx electrostatic potential profile analysis: ion, pH, steric, and charge effects. *Yale J. Biol. Med.* 61:427–446.
15. Ogston, A. G. 1958. The spaces in a uniform random suspension of fibres. *Trans. Faraday Soc.* 54:1754–1757.
16. Giddings, J. C., E. Kucera, C. P. Russell, and M. N. Myers. 1968. Statistical theory for equilibrium distribution of rigid molecules in inert porous networks. Exclusion chromatography. *J. Phys. Chem.* 72:4397–4408.
17. Serwer, P., and S. J. Hayes. 1981. Sieving of spherical viruses and related particles during electrophoresis in gels of agarose. *In* Electrophoresis '81. de Gruyter, Berlin. 237–243.
18. Serwer, P., J. L. Allen, and S. J. Hayes. 1983. Agarose gel electrophoresis of bacteriophages and related particles III. Dependence of gel sieving on the agarose preparation. *Electrophoresis.* 4:232–236.
19. Tietz, D., M. H. Gottlieb, J. S. Fawcett, and A. Chrambach. 1986. Electrophoresis on uncrosslinked polyacrylamide: molecular sieving and its potential applications. *Electrophoresis.* 7:217–220.
20. Tietz, D., and A. Chrambach. 1986. Analysis of convex Ferguson plots in agarose gel electrophoresis by empirical computer modeling. *Electrophoresis.* 7:241–250.
21. Tietz, D., and A. Chrambach. 1987. Computer simulation of the variable agarose fiber dimensions on the basis of mobility data derived from gel electrophoresis and using the Ogston theory. *Anal. Biochem.* 161:395–411.
22. Milner-White, J., and R. R. W. Poet. 1984. Computer graphics of large molecules. *Biochem. Soc. Trans.* 13:793–795.
23. Waki, S., J. D. Harvey, and A. R. Bellamy. 1982. Study of agarose by electron microscopy of freeze-fractured surfaces. *Biopolymers.* 21:1909–1926.
24. Brown, K. M., and J. E. Dennis. 1972. Derivative free analogues of the Levenberg-Marquardt and gauss algorithms for nonlinear least squares approximations. *Numerische Math.* 18:289–297.
25. Serwer, P., and S. J. Hayes. 1986. Exclusion of spheres by agarose gels during agarose gel electrophoresis: dependence on sphere's radius and the gel's concentration. *Anal. Biochem.* 158:72–78.
26. Laurent, T. C. 1967. Determination of the structure of agarose gels by gel chromatography. *Biochim. Biophys. Acta.* 136:199–205.
27. Serwer, P. 1983. Agarose gels: properties and use for electrophoresis. *Electrophoresis.* 4:375–382.
28. Barth, H. G. 1986. Characterization of water-soluble polymers using size-exclusion chromatography. Water soluble polymers. *Adv. Chem. Ser.* 213:31–55.